



Near-optimal Multiplier-Less Broadband Noise Shaping Filters

Hans Georg Brachtendorf¹ · Christoph Dalpiaz¹

Received: 12 April 2023 / Revised: 20 June 2023 / Accepted: 28 July 2023 / Published online: 31 August 2023
© The Author(s) 2023

Abstract

Noise shaping (NS) filters reduce the quantization noise power in one or more frequency band(s) while amplifying it in other bands. Narrow-band noise shaping filters are state of the art in audio signal processing, analog-digital and digital-analog conversion, direct digital synthesis, and other applications. However, it is much more difficult to design broadband NS filters. Since NS filters are used in feedback branches, they must therefore be designed direct path free which imposes a constraint on the filter coefficients. This constraint leads to prohibitive large filter coefficients employing state of the art filter design techniques.

This paper investigates the theoretical bound for NS filters and shows results about a novel design method for broadband FIR and IIR noise shaping filters and its multiplier-less hardware implementation. The method employed is a purely numerical approximation technique and leads to filter designs close to the discussed theoretical bound. The quantization of the filter coefficients is performed by a Canonical Signed Digit (CSD) representation of the coefficients. Two alternative architectures for the implementation of the filters are discussed. The design technique and the CSD quantization are realized in a MATLAB toolbox. The filters were moreover implemented in VHDL.

Keywords Broadband Noise Shaping Filters (NSF) · Multiplier-less NSF · Near-optimal design · Canonical Signed Digit (CSD) · VHDL implementation · Seamless design flow

1 Introduction

Noise shaping filters (NSF) are used, e.g., in digital-analog and analog-digital conversion. They virtually enlarge the wordlength of DACs and ADCs and hence their resolution. This makes them attractive in a variety of applications, such as audio signal processing [1–3], delta sigma converters [4–8] etc. In audio signal processing psychoacoustic noise shaping is widely used, e.g. [1–3], often in combination with dithering. These standard designs are narrow-band, requiring a large oversampling ratio (OSR). The large oversampling ratio however impairs the use of

NS filters to a broader class of applications. Essentially, one trades off bitwidth versus OSR. In [6, 7] the authors have proven that 1-bit delta sigma converters are in principle unperfectible and that distortion, limit cycles, instability, and noise modulation can never be totally avoided. The out-of-band gain is therefore a critical and limiting factor of NSF design for delta sigma converters. Moreover, they have shown that these shortcomings can in principle be circumvented by n -bit delta sigma converters with $n > 4$. Since n -bit converters are significantly more difficult to design for higher clock rates, broadband noise shaping filters enabling much smaller OSR are required.

The state of the art of NSF designs are focused on narrow-band filters for 1-bit delta sigma converters. Moreover, these papers lack of a discussion of implementation issues and implementation results. We conclude that there exists a shortcoming of design techniques for broadband NSFs which are proven to be close to the theoretical bounds. This paper deals therefore with the theoretical bounds of broadband NSF, their design and implementation. Toolboxes for a seamless design and hardware implementation in VHDL have been developed and will be discussed in this paper.

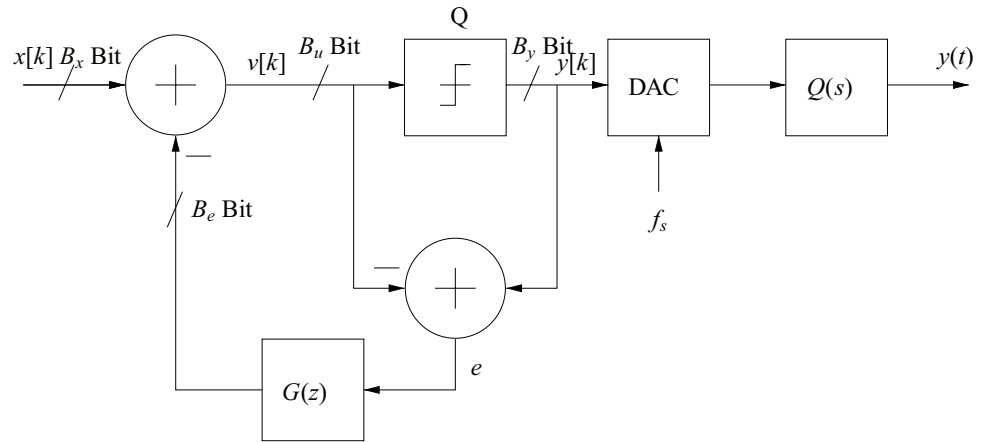
Christoph Dalpiaz contributed equally to this work.

✉ Hans Georg Brachtendorf
brachtd@fh-hagenberg.at

Christoph Dalpiaz
christoph.dalpiaz@fh-hagenberg.at

¹ Signal Processing Laboratory, University of Applied Sciences of Upper Austria, Softwarepark 11, Hagenberg 4232, Upper Austria, Austria

Figure 1 Noise shaping with quantizer Q.



2 Noise Shaping Filter Fundamentals

The Fig. 1 shows exemplarily a block diagram of a digital-analog conversion with noise shaping filter (NSF): the input signal x of wordlength B_x is converted to the analog domain by a DAC with wordlength $B_y < B_x$ and sampling rate f_s , requiring a quantization stage Q. The quantization error generated by the quantizer Q, $e[k] = y[k] - v[k]$, also referred to as quantization noise, is assumed to be a realization of a random white uniformly distributed stochastic process E . The noise shaping functionality comprises mainly a feedback path and filtering with transfer function $G(z)$ and noise transfer function (NTF) $H(z) = 1 - G(z)$ (e.g. [9]). Since $G(z) = 1 - H(z)$ must be direct path free, standard design techniques for digital filters cannot be applied.

We assume that $x[k]$ is a realization of a random process X . Let $\Phi_X(e^{j\Omega})$ be the power spectral density (PSD) of the stochastic process X . From the Wiener-Lee theorem the PSD of the filtered stochastic process, filtered by the impulse response $h[k]$ and transfer function $H(e^{j\Omega})$, is given by

$$\Phi_Y(e^{j\Omega}) = \Phi_X(e^{j\Omega}) |H(e^{j\Omega})|^2$$

i.e., the noise spectrum is shaped by $|H(e^{j\Omega})|^2$. NS filters are consequently designed in such a way that the magnitude response is small in the frequency bands of interest.

In what follows, we consider IIR noise shaping filters of order N with noise transfer function

$$H(z) = \frac{\sum_{m=0}^N b_m z^{-m}}{\sum_{n=0}^N a_n z^{-n}} = \frac{B(z^{-1})}{A(z^{-1})} \tag{1}$$

Let $H(z)$ be the transfer function of a stable and minimal phase filter, i.e. all roots of the polynomials of $B(z^{-1})$ and

$A(z^{-1})$ lie within the unit circle, then from Jensen’s formula [10] one obtains

$$\int_{-\pi}^{\pi} \ln |H(e^{j\Omega})|^2 d\Omega = 2\pi \ln \left| \frac{b_0}{a_0} \right|^2 \tag{2}$$

Since for noise shaping filters the transfer function $G(z)$ must be direct path free, the requirement $a_0 = b_0$ must hold for the NTF $H(z) = 1 - G(z)$. W.l.o.g. we impose the constraint $a_0 = b_0 = 1$, i.e. monic polynomials $A(z^{-1})$ and $B(z^{-1})$.

Hence (2) reads

$$\int_{-\pi}^{\pi} \ln |H(e^{j\Omega})|^2 d\Omega = 0 \tag{3}$$

This theorem implies that the total shaped noise power is always larger than the input noise power if the quantization noise is a white noise process, since a noise reduction in one frequency band trades off for a noise amplification in another one on a logarithmic scale.¹ The best what can be achieved is a piecewise constant absolute value of the transfer function, i.e., a constant reduction of the quantization noise power in the passband and a constant amplification in the stopbands. This is illustrated in Fig. 2 for a signal bandwidth of a quarter of the Nyquist frequency. The out-of-band gain is a critical factor for delta sigma converters which must be limited to guarantee stability.

This constraint $a_0 = b_0 = 1$ leads furthermore to prohibitively large absolute values of the remaining a and b coefficients employing state of the art filter design techniques when large bandwidths are required. Results suggest that absolute values of filter coefficients larger than 10^3 or even 10^4 occur.

¹ A similar result has been obtained in [11] as reported in [2, 7], referred to as Gerzon-Craven theorem.

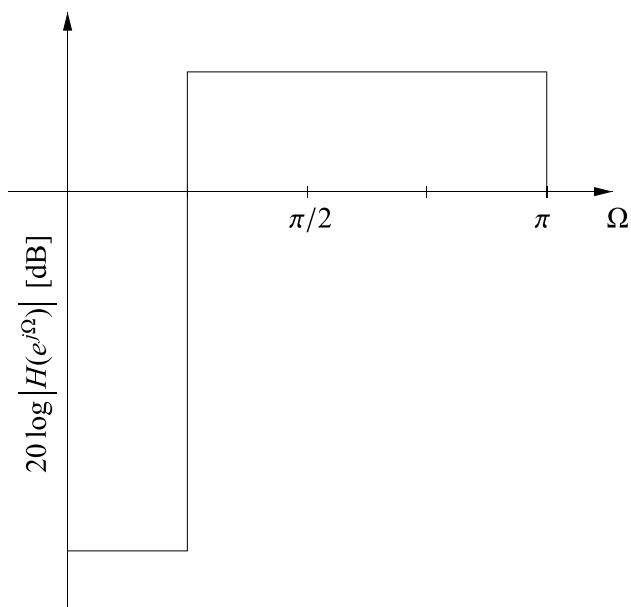


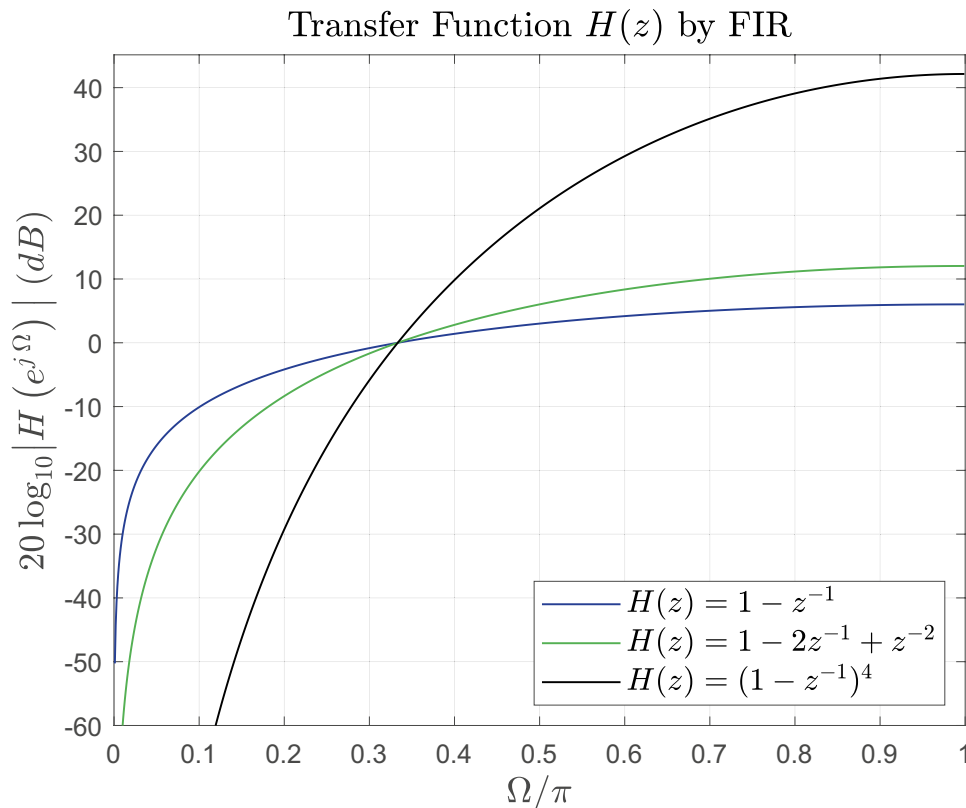
Figure 2 Illustration of the noise shaping theorem: optimal magnitude response of the noise shaping filter for a signal bandwidth of a quarter of the Nyquist frequency. The integral is constrained to zero.

3 Related Work

There exist multiplier-less narrow-band NSF of FIR type, which are employed in audio signal processing with noise transfer functions $H(z) = 1 - z^{-1}$ and $H(z) = 1 - 2z^{-1} + z^{-2}$, and others. In [12] the former transfer function has been generalized to a k th order pole, i.e., $H(z) = (1 - z^{-1})^k$, for use in a direct digital frequency synthesizer. This generalization leads to a narrow-band NSF too. Figure 3 depicts the magnitude responses. These FIR filters are extremely narrow-band, requiring a sample rate f_s significantly larger than the Nyquist rate. Even the $k = 4$ th pole filter requires an OSR of approximately 10 and is therefore constraint efficient for the synthesizer architecture described in [12].

Pavan et al. [4], Schreier [13], Schreier et al. [14] developed a sophisticated MATLAB toolbox [13, 14] for the design of NSFs for 1 bit delta sigma modulators. Though designed for large over sampling ratios, the core functions `synthesizeNTF` and `synthesizeChebyshevNTF` may be used for broadband NSFs as well. The results shown below (Figs. 4 and 5) choose an OSR of two, i.e., NSFs with a band width of up to half the Nyquist frequency.

Figure 3 Magnitude responses of a narrow-band NTFs.



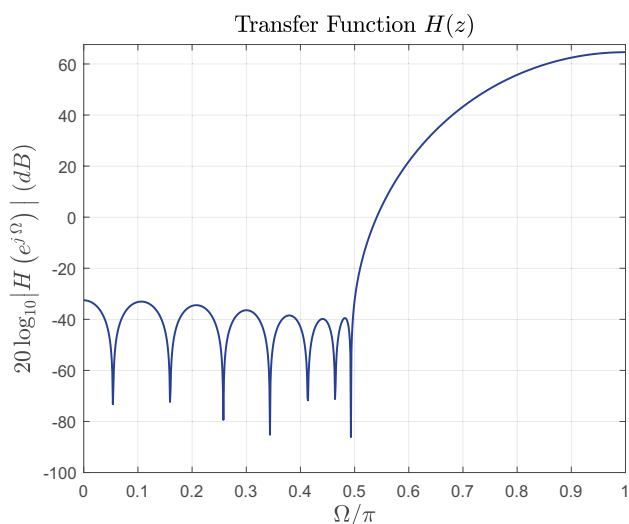
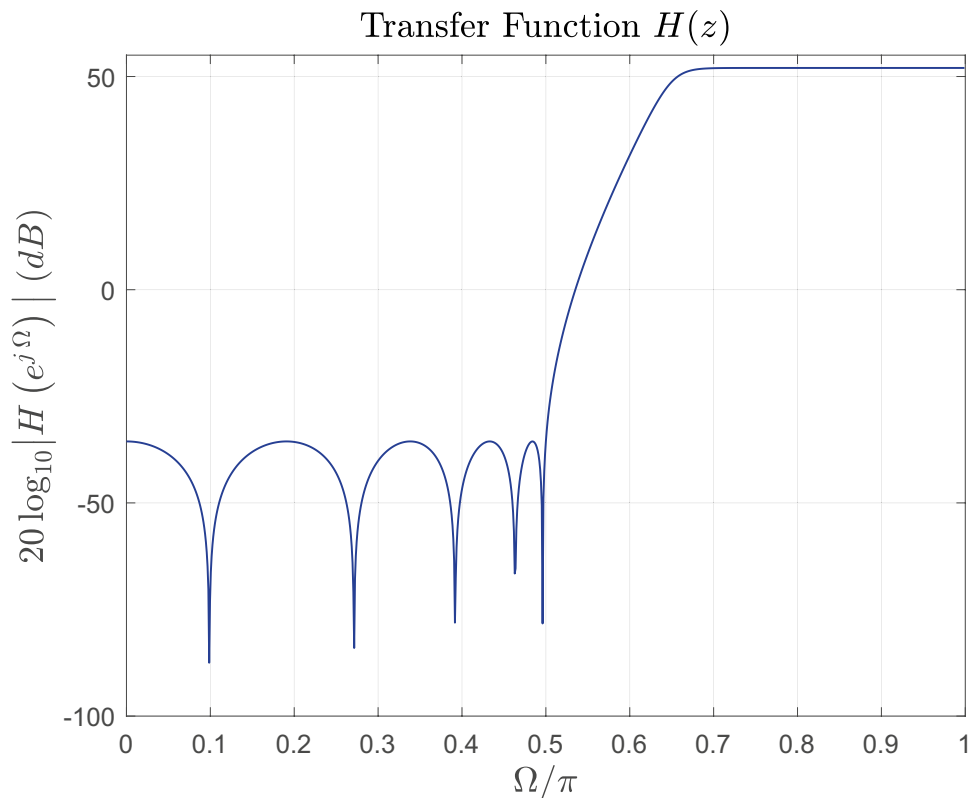


Figure 4 Magnitude response of a broadband $N = 14$ NTF according to [4] employing `synthesizeNTF`.

Since the NTF is not optimized outside the passband, one obtains an overly large amplification of the total noise power. Exemplarily, an $N = 14$ IIR NTF is depicted in Fig. 4, employing the `synthesizeNTF` function. The

Figure 5 Magnitude response of a broadband $N = 10$ Chebyshev type NTF according to [4] employing `synthesizeChebyshevNTF`.

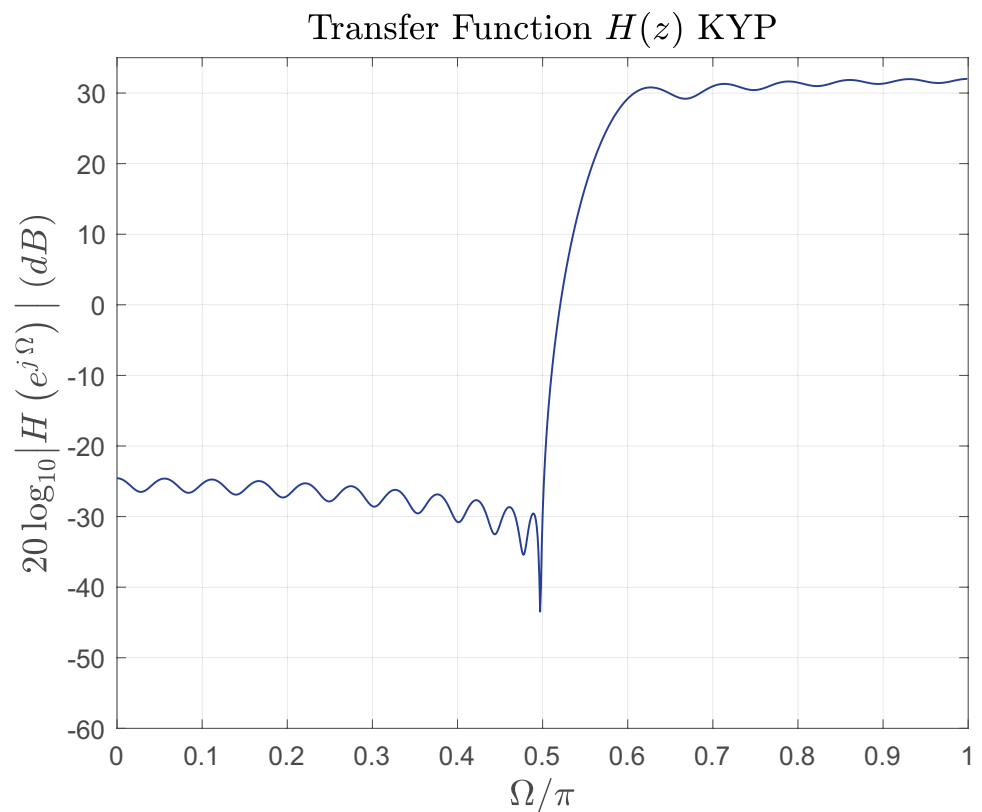


inband quantization noise reduction is > 32 dB whereas the out of band gain is up to about 65 dB. The Chebyshev filter designed with `synthesizeChebyshevNTF` as shown in Fig. 5 leads to an improved design: larger than 36 dB inband noise reduction and about 52 dB outband noise amplification. Nevertheless, both design methods are far from optimality as discussed in the previous section. Clearly, these functions are developed for delta sigma ADCs and DACs with large OSR.

Wannamaker [2] proposed a design method for psychoacoustically optimized FIR NSF filters. Firstly, the NSF with magnitude response $|H(e^{j\Omega})|^2$ is designed from the inverse of the psychoacoustically devised weighting function, fulfilling the Gerzon-Craven theorem [11]. Then a minimum phase filter $H(e^{j\Omega})$ is calculated from the squared magnitude response and finally the impulse response evaluated by an inverse FFT. The bottleneck of this technique is of course the numerical calculation of the minimal phase filter from the given magnitude response.

As noted in the previous section, the out-of-band gain is a critical factor for the stability of delta sigma converters and must be incorporated in the design process. This leads to a constraint optimization. In [5, 8, 15] the Kalman-Yakubovich-Popov (KYP) lemma has been used to this

Figure 6 Magnitude response of a broadband $N = 32$ FIR filter [8] employing NTF_MINMAX.



end applying the H_∞ norm. The constraint optimization problem has been recast into a symmetric eigenvalue problem which is iteratively solved using interior point methods. These standard designs are narrow-band, requiring a large oversampling ratio (OSR). The large oversampling ratio however impairs the use of NS filters to a broader class of applications. Nagahara and Yamamoto [8] provide the function NTF_MINMAX for solving the min-max less resulting from the KYP method. The Fig. 6 shows results for an OSR of two, employing an $N = 32$ FIR filter. The noise reduction is of about 24 dB and the out of band gain about 33 dB. Interestingly the algorithm performs worse for larger N and higher noise suppressions could not be achieved by parameter variations. We conclude that the design method employing the KYP lemma results also in suboptimal filter designs.

The challenges addressed in this paper are therefore

1. designing broadband noise shaping filters of a low filter order N ,
2. applicable for $n \geq 4$ bit delta sigma converters with moderate OSR,
3. with filter coefficients a, b being preferably single-digit decimal numbers, i.e. in $[-10, 10]$,
4. minimization of the overall noise growth outside the frequency band of interest, in view of the optimality constraint (3),
5. robust designs w.r.t. quantization of the filter coefficients,
6. hardware efficient multiplier-less implementation for high-speed signal processing.

This paper shows results of a novel design technique for broadband IIR NSF with minimal phase, which fulfills (3) and nearly piecewise constant noise transfer function. They are therefore close to the theoretical limit. Their filter coefficients are single-digit decimal numbers in most cases and therefore well suited for digital hardware implementation. The quantization is performed employing the Canonical Signed Digit representation [16] of the filter coefficients for a multiplier-less implementation of the filters. The signals are represented in a standard way by two's complement. Two alternative architectures for their hardware implementation are discussed. Special care has been taken for avoiding limit cycles of IIR filters using results from [17, 18].

4 Canonical Signed Digit Implementation

The filter coefficients are quantized employing the Canonical Signed Digit representation [16]. Firstly, the transfer function $H(z)$ is reformulated as a cascade of 1st and 2nd order filters in a standard manner, i.e.

$$H(z) = \prod_{p=1}^P \tilde{H}_p(z)$$

where $\tilde{H}_p(z)$ is either

$$\tilde{H}_p(z) = \frac{1 + b_1z^{-1}}{1 + a_1z^{-1}}, \quad \text{1st order}$$

or
$$\tilde{H}_p(z) = \frac{1 + b_1z^{-1} + b_2z^{-2}}{1 + a_1z^{-1} + a_2z^{-2}}, \quad \text{2nd order}$$

The 1st order rational polynomial is used when the pole and zero is on the real axis and the 2nd order rational polynomial otherwise in case of conjugate complex pairs. Alternatively, one may employ a parallel realization of the NTF, using partial fraction expansion. On the one hand, a parallel realization is less sensitive w.r.t. rounding errors due to quantization, on the other hand more operations are required compared with a cascade realization.

Quantization is most often done by using the two’s complement. Filter coefficients in $[-1, 1[$ are quantized by

$$a = -a_0 + \sum_{i=1}^{B-1} a_i 2^{-i}, \quad a_i \in \{0, 1\}$$

where a_0 is the sign bit and B the word length. The CSD representation instead quantizes the coefficients in the form

$$a = \sum_{i=1}^B a_i 2^{-i}, \quad a_i \in \{0, \pm 1\} \tag{4}$$

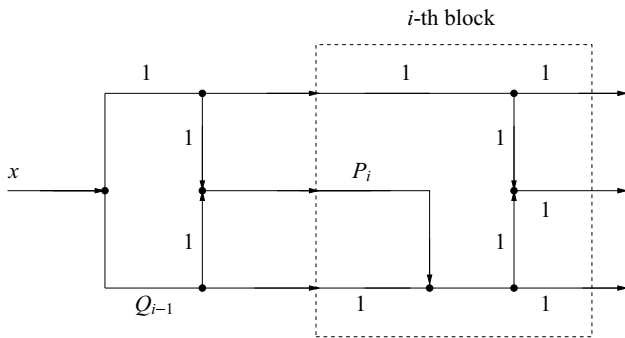


Figure 7 Signal flow graph of a 2 nd order block — 1st realization (P-block).

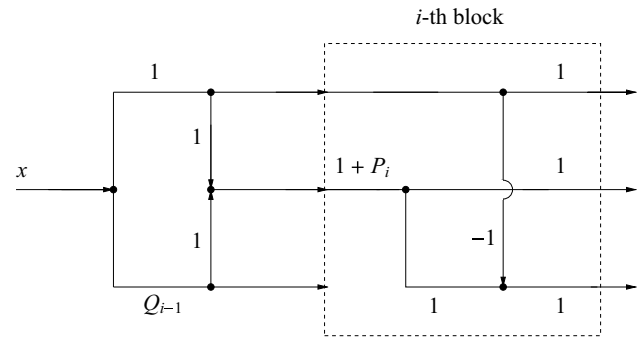


Figure 8 Signal flow graph of a 2 nd order block — 2nd realization (H-block).

The CSD representation is of advantage for a multiplier-less implementation of the filter, since in practical cases the number of nonzero digits is less compared with the two’s complement while fulfilling the design constraints. The second order sections of the architectures proposed in the next Section have been implemented using a minimum norm realization (e.g. [17]) and afterwards, the coefficients of the minimum norm realizations have been quantized using the CSD representation.

5 Broadband Noise Shaping Filters—Implementation

We propose below two alternative architectures of the NSF. Note that $G(z) = 1 - H(z)$ is direct path free and implemented in the feedback path of Fig. 1.

5.1 1st NSF Architecture

The NS filters are implemented in cascades of 1st and 2nd order blocks. To this end, we define

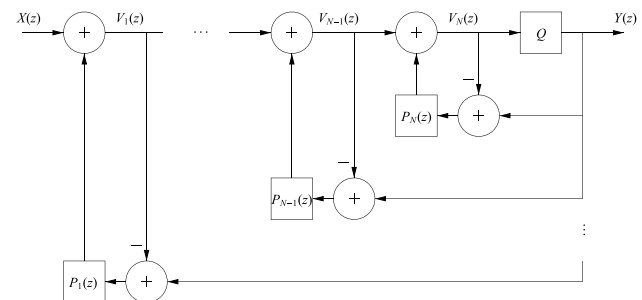


Figure 9 2nd NSF architecture [19].

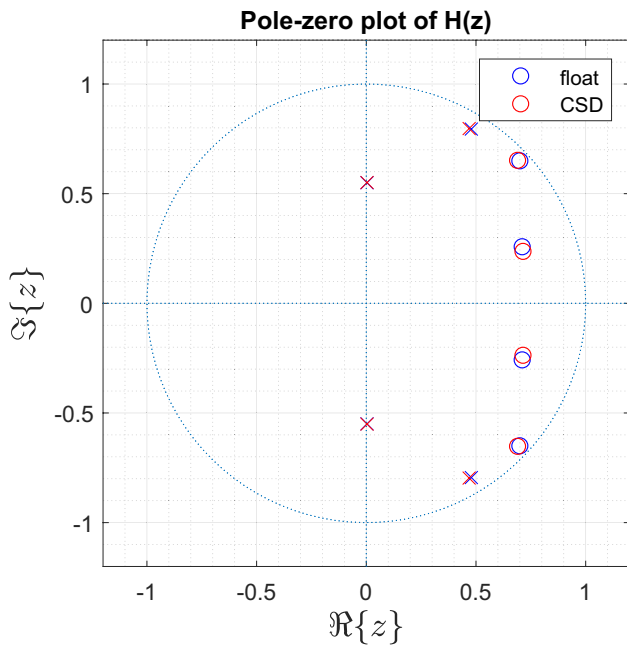
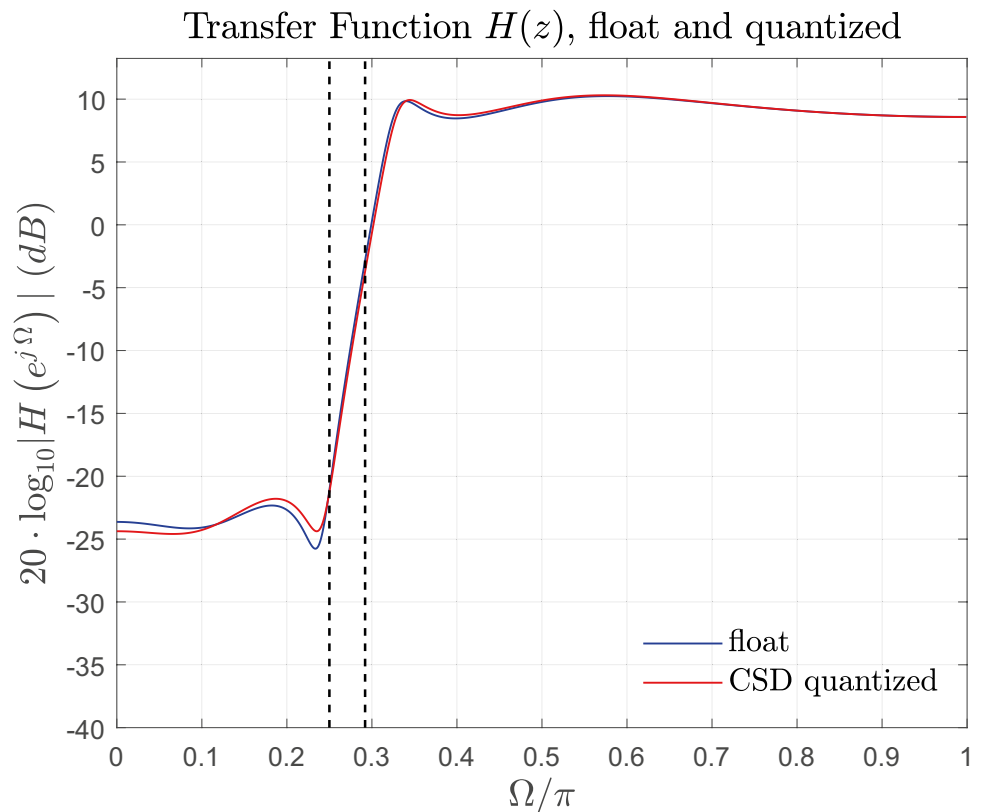


Figure 10 Pole-zero plot of NTF $H(z)$ with order $N = 4$ with float (blue) and CSD coefficients (red).

$$H_i(z) := \prod_{\ell=1}^i (1 + P_\ell(z)) =: 1 + Q_i(z), \quad i = 1, \dots, N \quad (5)$$

where $H(z) \equiv H_N(z)$, $G(z) \equiv -Q_N(z)$ and $P_\ell(z) = 1 - \tilde{H}_\ell(z)$.
We suggest alternatively the two 2-term recursions

Figure 11 Transfer function of NSF $H(z)$ with order $N = 4$ in float representation and quantized using CSD representation.



$$Q_i(z) = Q_{i-1}(z) + P_i(z)H_{i-1}(z) \quad (6)$$

$$Q_i(z) = (1 + P_i(z))(1 + Q_{i-1}(z)) - 1 \quad (7)$$

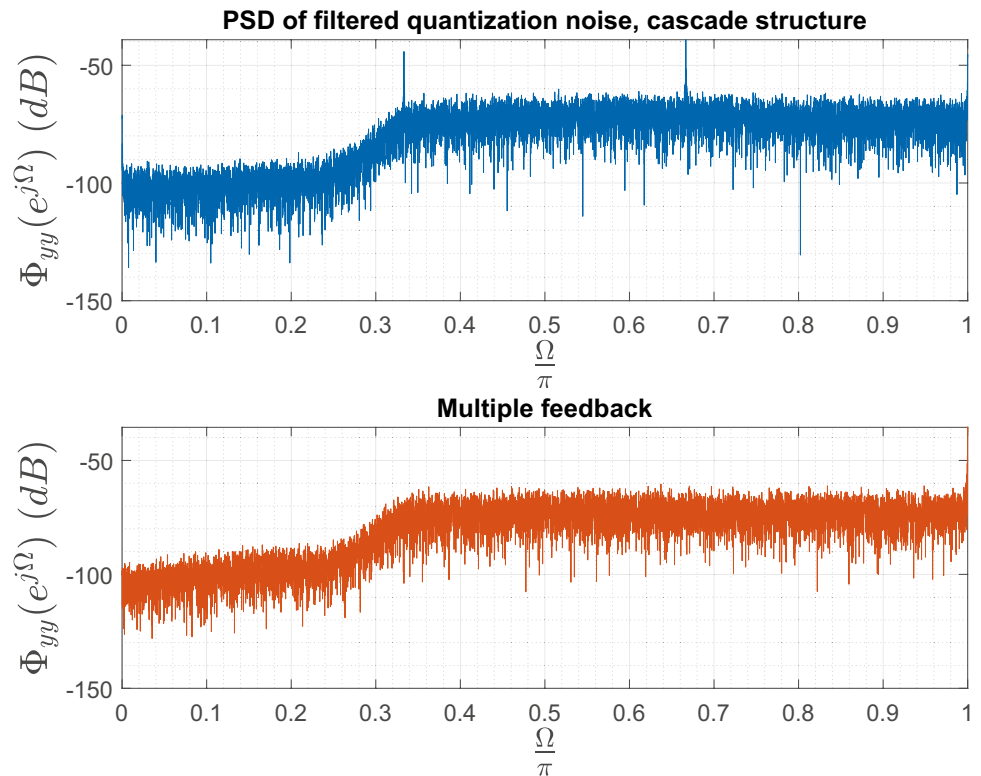
The signal flow graph for (6), referred to as P-block, is depicted in Fig. 7 and for (7), referred to as H-block, in Fig. 8. The realization by an H-block (7) is unlike (6) not direct path free, therefore at least one stage in the cascade must be a realization of a P-block (6), since a direct path free feedback loop is required.

5.2 2nd NSF Architecture

We consider the multiple feedback NSF architecture depicted in Fig. 9 [19]. By inspection, we have the recursive calculations

$$\begin{aligned} Y &= V_N + E \\ V_N &= V_{N-1} + P_N(z)(Y - V_N) = V_{N-1} + P_N(z)E \\ Y &= V_{N-1} + (1 + P_N(z))E \\ V_{N-1} &= V_{N-2} + P_{N-1}(z)(Y - V_{N-1}) \\ &= V_{N-2} + P_{N-1}(z)(1 + P_N(z))E \\ Y &= V_{N-2} + (1 + P_{N-1}(z))(1 + P_N(z))E \\ V_{N-2} &= V_{N-3} + P_{N-2}(z)(Y - V_{N-2}) \\ &= V_{N-3} + P_{N-2}(z)(1 + P_{N-1}(z))(1 + P_N(z))E \\ Y &= V_{N-3} + (1 + P_{N-2}(z))(1 + P_{N-1}(z))(1 + P_N(z))E \\ &\dots \end{aligned} \quad (8)$$

Figure 12 PSD of the filtered quantization noise of NSF architectures with order $N = 4$.



$$Y = X(z) + E \prod_{\ell=1}^N (1 + P_{\ell}(z)) \tag{9}$$

which implements recursively (5).

6 Broadband Noise Shaping Filters—Results

6.1 Implementation

The NSF architectures have been implemented in VHDL. Whereas the filter coefficients are quantized in the CSD representation, the signals instead in the two’s complement with b integer and B decimal bits in a standard manner. The second order systems $P_i(z)$ in Fig. 7 have been realized using a minimum norm realization (e.g. [17]) and the multiplication results are quantized with rounding to zero in order to avoid limit cycles [18]. The filters have been simulated with ModelSim - Intel FPGA Starter Edition 10.5b. The test signal is a frequency modulated

Chirp signal. The synthesis for the Intel Cyclone V FPGA 5CSEMA5F31C6 has been performed with Intel Quartus Prime Version 18.1.0 SJ Lite Edition. In the following sections, example filters including simulation and synthesis results are presented.

Table 1 Synthesis results of NSF architectures with order $N = 4$ for the Intel Cyclone V FPGA.

Architecture	ALM	ALUT	Registers	f_{max} [MHz]
Cascade structure	493	948	64	61.47
Multiple feedback	492	939	64	72.18

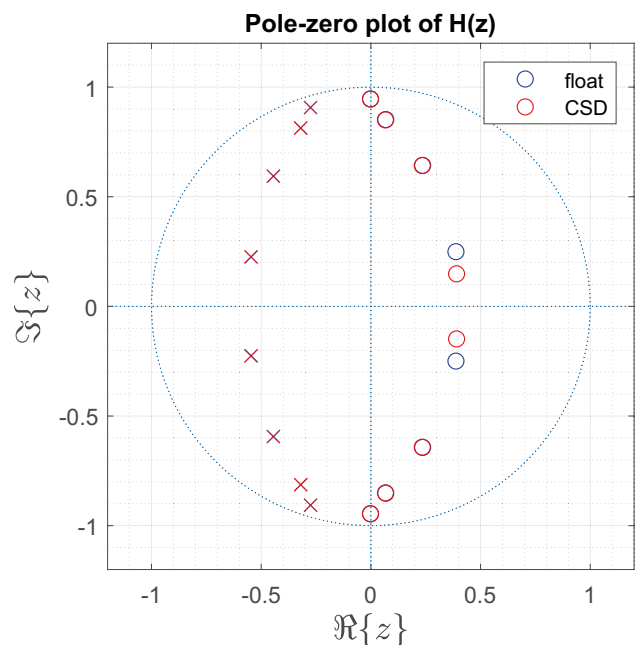
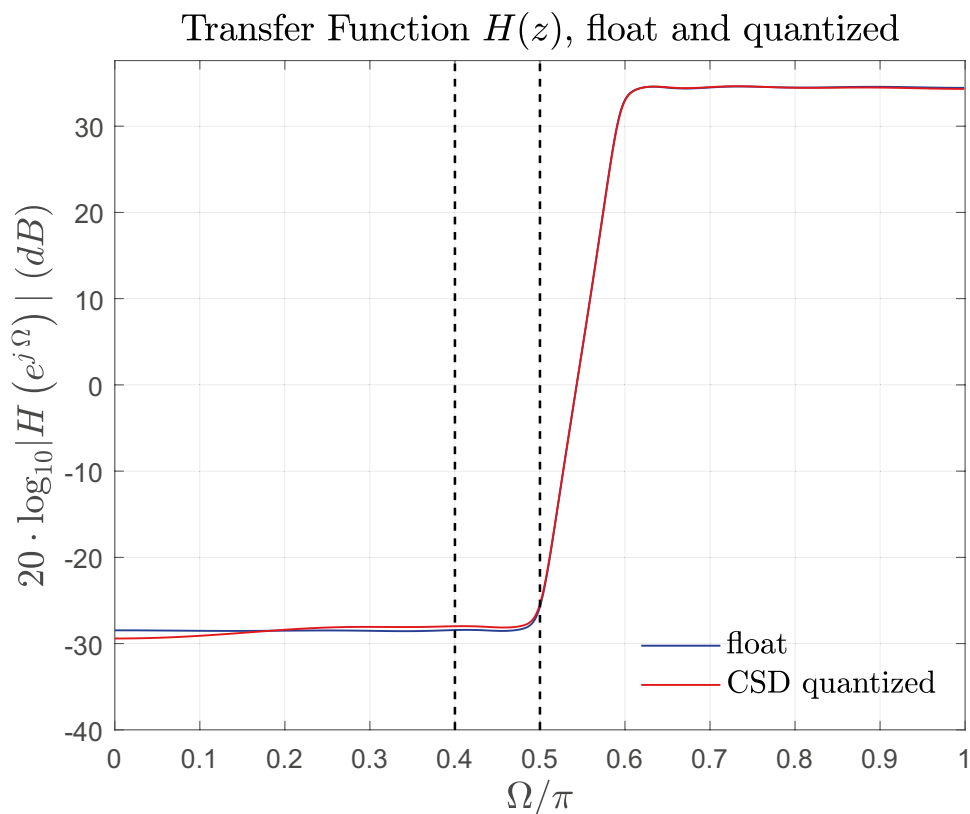


Figure 13 Pole-zero plot of NTF $H(z)$ with order $N = 8$ with float (blue) and CSD coefficients (red).

Figure 14 Transfer function of NSF with order $N = 8$ in float representation and quantized using CSD representation.

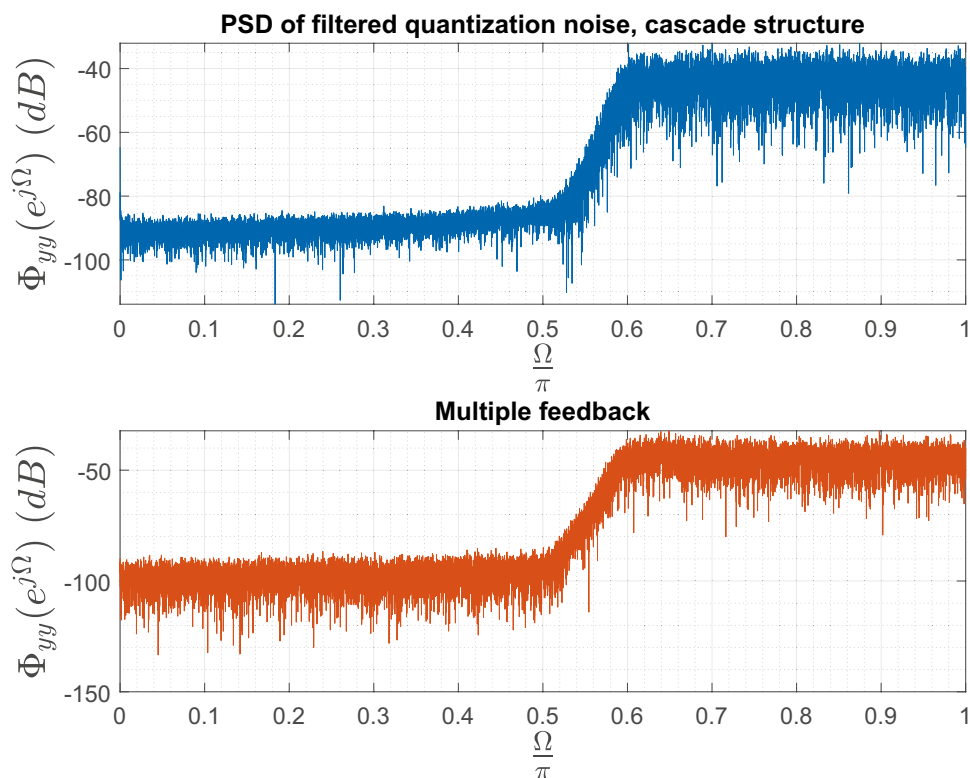


6.2 Noise Shaping Filter with Order $N = 4$

In the following, simulation and synthesis results of a 4th order IIR NSF are presented. The pole-zero plot of the NS filter is

depicted in Fig. 10 and the NTF in Fig. 11. For the quantization of the signals in two’s complement, one integer bit and fifteen decimal bits have been used. The PSDs of the filtered quantization noise in the hardware simulation is depicted in

Figure 15 PSD of the filtered quantization noise of NSF architectures with order $N = 8$.



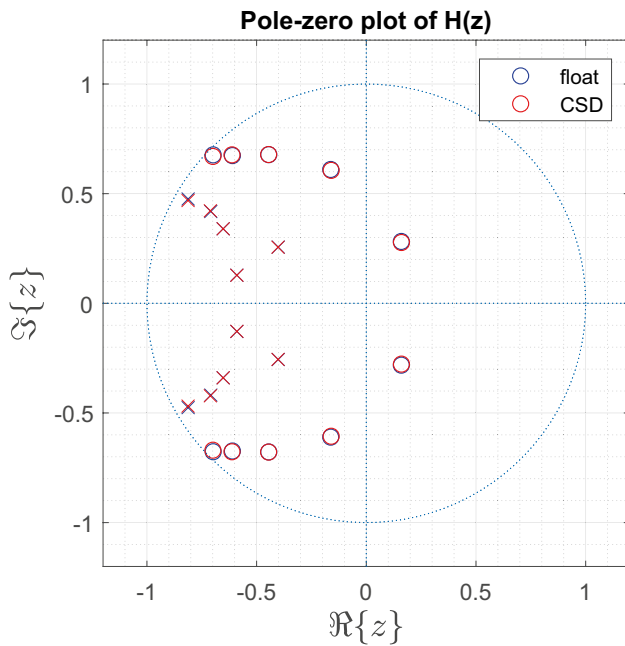


Figure 16 Pole-zero plot of NTF $H(z)$ with order $N = 10$ with float (blue) and CSD coefficients (red).

Fig. 12. The Table 1 depicts the maximum clock frequency and the resource utilization of adaptive logic modules (ALM), adaptive look-up tables (ALUT) and registers for the discussed architectures. The noise suppression operates for a bandwidth

Figure 17 Transfer function of NSF with order $N = 10$ in float representation and quantized using CSD representation.

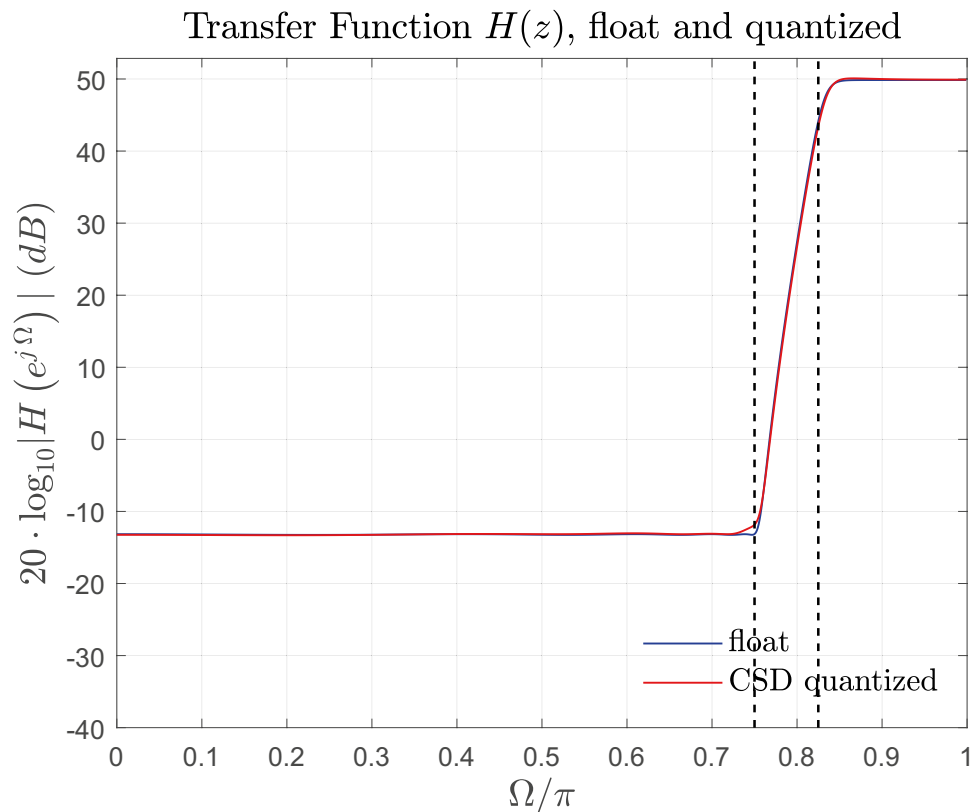


Table 2 Synthesis results of NSF architectures with order $N = 8$ for the Intel Cyclone V FPGA.

Architecture	ALM	ALUT	Registers	f_{max} [MHz]
Cascade structure	1063	2031	128	51.05
Multiple feedback	1075	2000	128	58.87

of about $B = \pi/4$, which is 25% of the total bandwidth. Comparing Fig. 11 with the optimal filter Fig. 2 one can see the excellent match despite the very low filter order.

6.3 Noise Shaping Filter with Order $N = 8$

In this Section, simulation and synthesis results of an 8th order NSF are presented. The pole-zero plot of the noise transfer function is depicted in Fig. 13 and the NTF in Fig. 14. As for the 4th order NSF, one integer bit and fifteen decimal bits have been used for the quantization of the signals. The PSD of the filtered quantization noise in the hardware simulation is depicted in Fig. 15 and Table 2 depicts the synthesis results. The noise suppression operates for a bandwidth of about $B = \pi/2$ (halfband).

6.4 Noise Shaping Filter with Order $N = 10$

In this Section, simulation and synthesis results of a 10th order NSF are presented. The pole-zero plot of the noise

Figure 18 PSD of the filtered quantization noise of NSF architectures with order $N = 10$.

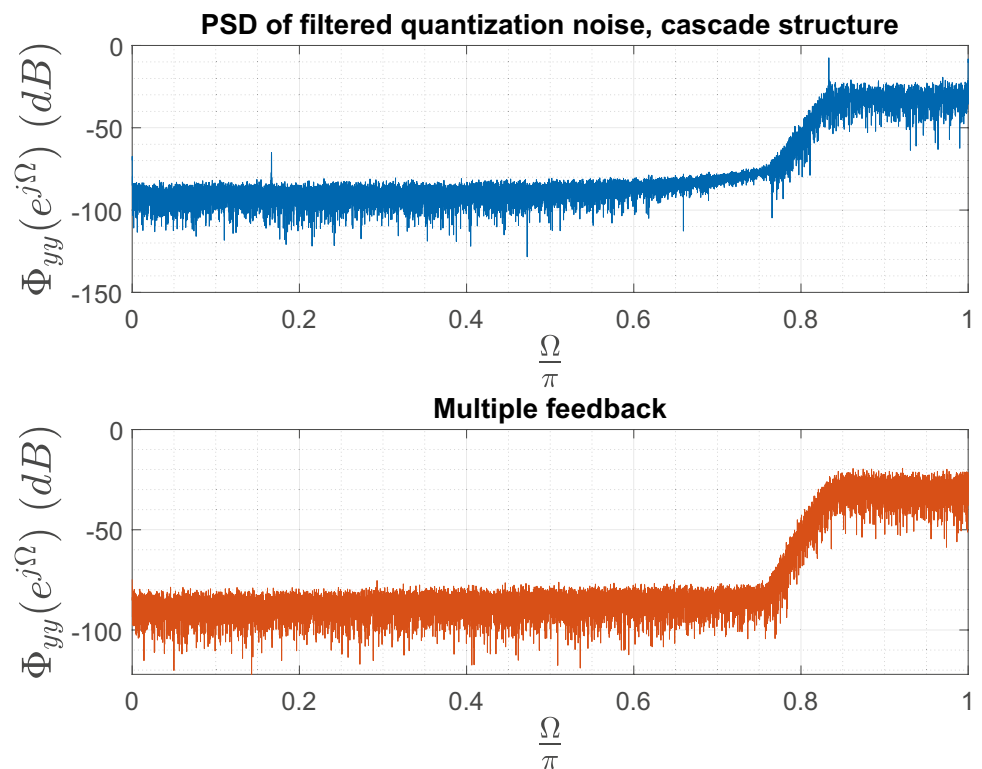


Table 3 Synthesis results of NSF architectures with order $N = 10$ for the Intel Cyclone V FPGA.

Architecture	ALM	ALUT	Registers	f_{max} [MHz]
Cascade structure	1514	2927	190	46.98
Multiple feedback	1558	2874	190	51.41

transfer function is depicted in Fig. 16 and the NTF in Fig. 17. For the quantization of the signals in two's complement, four integer bits and fifteen decimal bits have been used. The PSD of the filtered quantization noise in the hardware simulation is depicted in Fig. 18 and Table 3 depicts the synthesis results. The noise suppression operates for a bandwidth of about $B = 3\pi/4$, which is 75% of the total bandwidth. The transfer function Fig. 17 matches the optimality constraint for minimal phase NSFs nearly perfectly.

7 Conclusion

In this paper a seamless design flow for broadband noise shaping IIR filters has been described. The novel design technique features a near optimum transfer characteristic, i.e. adjustable noise suppression in the frequency range of interest and simultaneously low noise growth in the remaining frequency bands. The filters are close to the theoretical bound as discussed in this paper. The filter coefficients

of the transfer function are typically single digit decimal numbers and hence well suited for a realization in a digital circuit. The filters are moreover implemented multiplier-less. Two alternative architectures have been discussed in detail. The filter coefficients are quantized employing the Canonical Signed Digit (CSD) representation. CSD leads in practical cases to less nonzero digits compared with the usual two's complement, enabling less hardware resources, less power consumption and higher clock rates.

The design flow comprises a toolbox for the design of the filter, quantization of the filter coefficients in the cost-efficient CSD format and an automated generation of a VHDL package containing the filter parameters.

The noise shaping filters can be realized for low- and highpass, bandpass and bandstop signals. In this paper only cases for lowpass signals have been discussed. Alternatively, a design technique for FIR noise shaping filters has been developed. Results on their multirate implementation will be considered in another paper.

Acknowledgements The authors would like to thank M. Holters and U. Zölzer for fruitful discussions on the theoretical bounds of noise shaping filters.

Funding Open access funding provided by University of Applied Sciences Upper Austria. This project AMOR ATCZ203 has been cofinanced by the European Union using financial means of the European Regional Development Fund (INTERREG) for sustainable cross border cooperation. Further information on INTERREG Austria-Czech Republic is available at <https://www.at-cz.eu/at.interreg>

Declarations

Competing Interests The authors do not have any competing interests.

Open Access This article is licensed under a Creative Commons Attribution 4.0 International License, which permits use, sharing, adaptation, distribution and reproduction in any medium or format, as long as you give appropriate credit to the original author(s) and the source, provide a link to the Creative Commons licence, and indicate if changes were made. The images or other third party material in this article are included in the article's Creative Commons licence, unless indicated otherwise in a credit line to the material. If material is not included in the article's Creative Commons licence and your intended use is not permitted by statutory regulation or exceeds the permitted use, you will need to obtain permission directly from the copyright holder. To view a copy of this licence, visit <http://creativecommons.org/licenses/by/4.0/>.

References

- De Koning, D., & Verhelst, W. (2003). On psychoacoustic noise shaping for audio requantization. In: *2003 IEEE International Conference on Acoustics, Speech, and Signal Processing, 2003. Proceedings. (ICASSP '03)* (vol. 5, p. 453). <https://doi.org/10.1109/ICASSP.2003.1200004>
- Wannamaker, R. (1992). Psychoacoustically optimal noise shaping. *Journal of the Audio Engineering Society*, *40*, 611–620.
- Dunn, C., & Sandler, M. (1997). Psychoacoustically optimal sigma-delta modulation. *Journal of the Audio Engineering Society*, *45*, 212–223.
- Pavan, S., Schreier, R., & Temes, G. C. (2017). Understanding Delta-Sigma Data Converters. *IEEE Press Series on Microelectronic Systems*. Wiley, Hoboken, NJ.
- Callegari, S., & Bizzarri, F. (2015). Optimal design of the noise transfer function of $\delta\sigma$ modulators: IIR strategies, FIR strategies, FIR strategies with preassigned poles. *Signal Processing*, *114*, 117–130. <https://doi.org/10.1016/j.sigpro.2015.02.001>
- Vanderkooy, J., & Lipshitz, S. P. (2001). Why 1-bit sigma-delta conversion is unsuitable for high-quality applications. *Journal of The Audio Engineering Society*.
- Lipshitz, S. P., Vanderkooy, J., & Wannamaker, R. A. (1991). Minimally audible noise shaping. *Journal of the Audio Engineering Society*, *39*(11), 836–852.
- Nagahara, M., & Yamamoto, Y. (2012). Frequency domain min-max optimization of noise-shaping delta-sigma modulators. *IEEE Transactions on Signal Processing*, *60*(6), 2828–2839. <https://doi.org/10.1109/TSP.2012.2188522>
- Zölzer, U. (2022). *Digital Audio Signal Processing* (2nd ed.). Hoboken, NJ: Wiley.
- Holters, M. *Optimal Noise Shaping Filters*. Private communication.
- Gerzon, M. A., & Craven, P. G. (1989). Optimal noise shaping and dither of digital signals. *Journal of the Audio Engineering Society (Abstracts)*, *37*, 1072. Preprint 2822.
- Dai, F. F., Ni, W., Yin, S., & Jaeger, R. C. (2006). A direct digital frequency synthesizer with fourth-order phase domain $\Delta\Sigma$ Sigma/noise shaper and 12-bit current-steering DAC. *IEEE Journal of Solid-State Circuits*, *41*(4), 839–850. <https://doi.org/10.1109/JSSC.2006.870749>
- Schreier, R. (2011). Thedelta-sigmatoolbox. Technical report, The Delta-Sigma Toolbox Analog Devices, Release 7.4. <http://www.mathworks.com/matlabcentral/fileexchange/19-delta-sigma-toolbox>
- Schreier, R., Pavan, S., & Temes, G. (2017). *The Delta-Sigma Toolbox*. (pp. 499–537). <https://doi.org/10.1002/9781119258308.app2>
- Li, X., Yu, C. B., & Gao, H. (2014). Design of delta-sigma modulators via generalized kalman-yakubovich-popov lemma. *Automatica*, *50*(10), 2700–2708. <https://doi.org/10.1016/j.automatica.2014.09.002>
- Hewlett, R. M., & Swartzlantler, E. S. (2000). Canonical signed digit representation for FIR digital filters. In: *2000 IEEE Workshop on Signal Processing Systems. SiPS 2000. Design and Implementation (Cat. No.00TH8528)* (pp. 416–426). <https://doi.org/10.1109/SIPS.2000.886740>
- Barnes, C., & Fam, A. (1977). Minimum norm recursive digital filters that are free of overflow limit cycles. *IEEE Transactions on Circuits and Systems*, *24*(10), 569–574. <https://doi.org/10.1109/TCS.1977.1084275>
- Bauer, P. H., & Leclerc, L.-J. (1991). A computer-aided test for the absence of limit cycles in fixed-point digital filters. *IEEE Transactions on Signal Processing*, *39*(11), 2400–2410. <https://doi.org/10.1109/78.97995>
- Lopes, P. A. C., & Gerald, J. A. B. (2021). Low delay short word length sigma delta active noise control. *IEEE Transactions on Circuits and Systems I: Regular Papers*, *68*(9), 3746–3757. <https://doi.org/10.1109/TCSI.2021.3096180>

Publisher's Note Springer Nature remains neutral with regard to jurisdictional claims in published maps and institutional affiliations.



Hans Georg Brachtendorf graduated in Electrical Engineering from RWTH Aachen, Germany in 1989 and obtained the Ph.D. degree from the University of Bremen at the Institute for Electromagnetic Theory and Microelectronics in 1994, also in Electrical Engineering. From 1994–2001 he was an Assistant Professor (C1) also at the University of Bremen and obtained the Venia Legendi (Habilitation) from the same university in 2001. In 1997–1998 he was affiliated with the

Wireless Laboratory of Bell Laboratories/Lucent Technologies in Murray Hill/New Jersey, where he performed research in circuit simulation and design. In 2001 he joined the Fraunhofer Institute for Integrated Circuits in Erlangen, Germany. His focus there was on system design and simulation for satellite broadcasting systems and transceiver designs. Since 2005 Dr. Brachtendorf is full professor at the University of Applied Science of Upper Austria for System Design and Simulation, Communications and Signal Processing. His research interests include circuit design, modelling and simulation as well as signal processing and digital communication.



Christoph Dalpiaz received the B.Sc. degree in Hardware-Software-Design from the University of Applied Sciences Upper Austria in 2022. He is currently studying in the master's degree program Embedded Systems Design at the University of Applied Sciences Upper Austria. He worked in the Signal Processing Lab at the University of Applied Sciences Upper Austria on topics in Digital Signal Processing and Digital Communications.